Extreme Mechanics Letters 62 (2023) 102032

Contents lists available at ScienceDirect

Extreme Mechanics Letters

journal homepage: www.elsevier.com/locate/eml

Coiling an optical fiber for long-range dynamic displacement and force sensing

Yu-Han Wang [a], Zhu-Long Xu [a], Yong Wang [a], Ronghua Huan [a], Hanqing Jiang [b], Kuo-Chih Chuang [a,*]

[a] Key Laboratory of Soft Machines and Smart Devices of Zhejiang Province, School of Aeronautics and Astronautics, Institute of Applied Mechanics, Zhejiang University, Hangzhou, 310027, China
[b] School of Engineering, Westlake University, Hangzhou, 310024, China

ARTICLE INFO

Article history:
Received 7 April 2023
Received in revised form 10 May 2023
Accepted 22 May 2023
Available online 7 June 2023

Keywords:
optical fibers
Bending loss
Tendril coiling
Kresling

ABSTRACT

Optical fiber sensors have been applied on detecting various physical parameters. In this work, inspired by the mechanism of tendril coiling, we designed a spring-like sensor using optical fibers based on macro bending loss. The proposed optical-fiber spring has good elasticity like a mechanical spring and thus can be used to measure large displacement. As a contact-type sensor, the fabricated optical-fiber spring can measure dynamic displacement, whose range is 4 orders of magnitude higher than that of the point-wise fiber Bragg grating displacement sensor. In addition to the point-wise displacement sensing, we further integrated the optical-fiber spring with a *Kresling* origami to form a force sensor.

1. Introduction

Not limited to animals, various plants in nature can be excellent sources of inspiration for scientists and engineers to design robots, actuators, or sensors. For plants, different growth of plant tissues can lead to morphogenesis, by which various parts of functional organs, such as roots, stems, or leaves, can be formed. Inhomogeneous and nonuniform growth in various parts of plant organs can lead to mismatched growth strain and from which a wide variety of plant configuration such as tendril coiling can be formed [1–4]. Take the formation of climbing plants such as cucumber tendrils for example, by asymmetric contraction of the plant tissues, the tendril coil is formed where the lignified fiber on the ventral side contracts longitudinally with respect to that on the dorsal side [5]. Since both ends of the tendril are clamped, the asymmetrical contraction of the stiffer fiber with respect to the surrounding soft tendril tissue as well as the prevention of twisting at the two ends impose a topological constraint which accounts for the local bending and the curvature of the overall tendril coiling. Interestingly, since the total twist in the tendril is conservative, two connected helices with opposite chirality, separated only by a small segment, will exist in the tendril coil [6]. Despite not being a perfect coil with only one chirality, the tendril coil, with a spring-like configuration which store elastic energy while possessing large deformation, can inspire the sensor design where long-range and tunable sensing range might be achieved.

To realize the double-chirality "spring", a common approach is to pre-stretch a straight elastic strip and then fix it to another traction-free straight elastic strip. By releasing the prestress while keeping the two ends not rotating, the elastic composite strip will form a spring-like coil with two connected opposite-handed helices. If the prestress exceeds a critical value, the initial linear configuration will spontaneously form a spiral with the presence of twists [7–10]. The spiral composite has been used in many fields [11–17]. However, to the best of the authors' knowledge, the spiral composite has not been applied to design optical fiber sensors.

Due to their advantages such as small size, immunity to electromagnetic field, and no requirement of electrical power at the sensing point, optical fibers provide a route for designing sensors in various applications. Optical fiber-based sensors, such as fiber Bragg gratings (FBGs), have been utilized for years to measure various physical quantities (e.g., strain [18–21], temperature [22–24], force [25,26], pressure [27,28], or displacement [29–31]). Despite possessing very high sensitivity, the sensing range of the pointwise FBG displacement sensors is small. When a fiber is bent, power loss of light occurs where light is lost from the core by radiation [32]. The bending loss of light is sensitive to the curvature of the fiber and thus change of the curvature can be applied in sensing. If the formation mechanism of the tendril coils can be borrowed for generating the spiral configuration on the fiber, not only the bending loss can be amplified, the sensing

* Corresponding author.
E-mail address: chuangkc@zju.edu.cn (K.-C. Chuang).

https://doi.org/10.1016/j.eml.2023.102032
2352-4316/

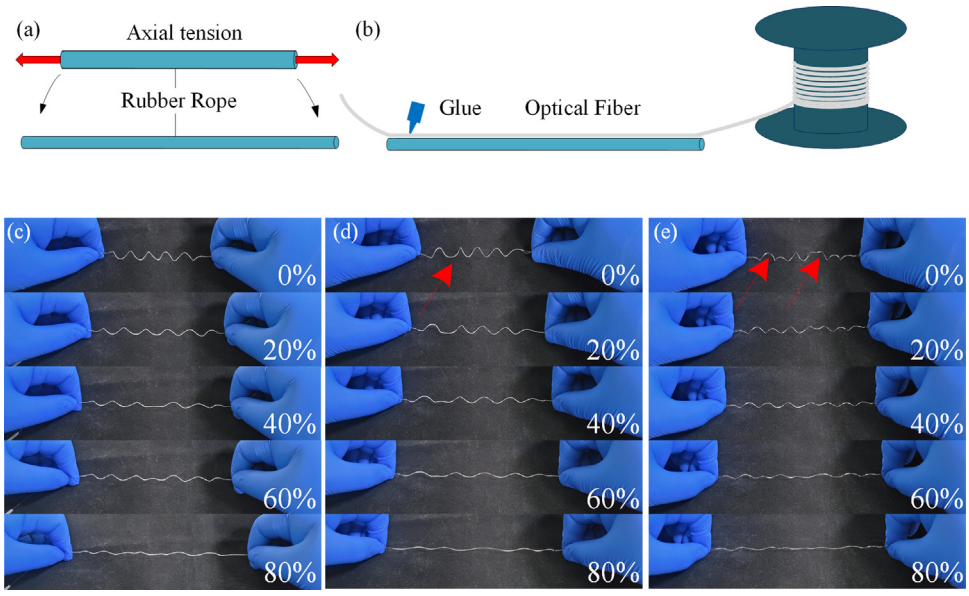

Fig. 1. (a-b) Fabrication process of the optical-fiber spring. (c-e) Morphological changes in the optical-fiber spring during stretching.

range can be tuned and enlarged by controlling the degree of the spiral.

2. Material and methods

In order to make the configuration of an optical fiber sensor like that of a tendrils coil, which we will refer to as an optical-fiber spring in this letter, we combined a thin round rubber rope and an optical fiber to form a bilayer fiber-rope composite. The optical fiber, whose Young's modulus is 72 GPa, behaves as a stiff fiber band. The rubber rope, whose Young's modulus is less as 10 MPa, behaves as the surrounding soft tendril tissue of the cucumber tendrils. Borrowing from the asymmetric contraction, the method to generate the spiral configuration is to prestretch the easily-deformed elastic rope and glue it to the undeformed straight optical fiber. The prestress is then released while keeping both ends of the composite not rotating, the intrinsic curvature in the spiral bilayer fiber-rope composite will be generated. In our work, a short rubber rope with an initial length of 10 cm and a diameter of 0.5 mm was stretched to be 18 cm long and then a 40 cm-long optical fiber was bonded to the stretched rubber rope. Specifically, a primer (770, aliphatic amine) was applied on both the surface of the tensioned rubber rope and the optical fiber before bonding them together with an instant adhesive glue (401, ethyl cyanoacrylate). The fabrication process is illustrated in Fig. 1a and b. Then, the prestress was gradually released without rotating the two holding ends and out-of-plane bending and twists will occur in the optical-fiber spring. Fig. 1c–e show the different morphology, where Fig. 1d shows the most common single twist model when both ends are kept not rotating during the shrinkage process. From Fig. 1c–e, where the stretch of the optical-fiber spring is marked, the connected helices with opposite chiralities can be observed, despite that the "perversion" is not in the middle of the optical-fiber spring due to the fact that a perfect bonding and releasing is not easily achieved. From the perspective of mechanics, the presence of the connected opposite chirality can be explained by the reduction of the total elastic energy while satisfying the boundary conditions [33–38].

After shrinking, the optical-fiber spring can still be stretched to a near-straight state, as shown in Fig. 1c–e. In the stretching process, the bending loss of the optical power gradually decreases and this can be utilized to measure the relative displacement between the two ends of the optical-fiber spring. Through a photodiode, the optical signal is converted into electrical signal, showing monotonically increasing as shown in Fig. 2 and the response can be regarded as having two linear sensing regions, marked as light blue (i.e., low displacement sensitivity 0.0471 V/mm but with a large sensing range of 20 mm, where the value of the coefficient of determination (R^2) is 0.9764) and light yellow (i.e., higher displacement sensitivity 0.57 V/mm but with a smaller sensing range of 10 mm, where R^2 is 0.9937), respectively. The two sensing sensitivities might be caused due to several factors, including a nonlinear relationship between the bending curvature and the loss of light, a nonlinear variation of the curvature with respect to the tension, and a slightly overwinding behavior (see [5]). During the shrinkage process, due to different boundary conditions, non-twist, single twist, and multiple twists might also occur (see Supplement 1 for the discussions of their performances as sensors).

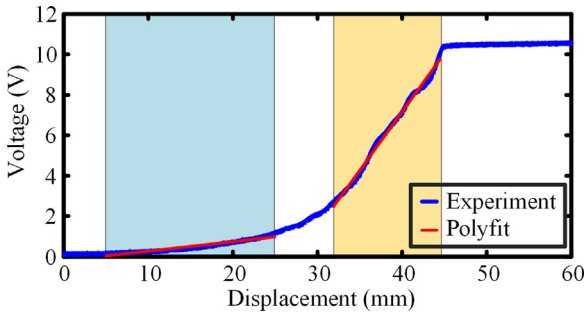

Fig. 2. Changes in the electrical signal converted by the photodiode during the stretching and contraction of the optical-fiber spring sensor. . (For interpretation of the references to color in this figure legend, the reader is referred to the web version of this article.)

If one end of the optical-fiber spring is fixed to a surface point of a structure or a movable mechanical device, the relative displacement between the two ends of the optical-fiber spring can become a pointwise displacement. As a contact-type sensor, from Fig. 2 we can see that the displacement measuring range of the fabricated optical-fiber spring is about 20 mm, which is 4 orders of magnitude higher than that (i.e., 2000 nm) of the pointwise fiber Bragg grating (FBG) displacement sensor, when the

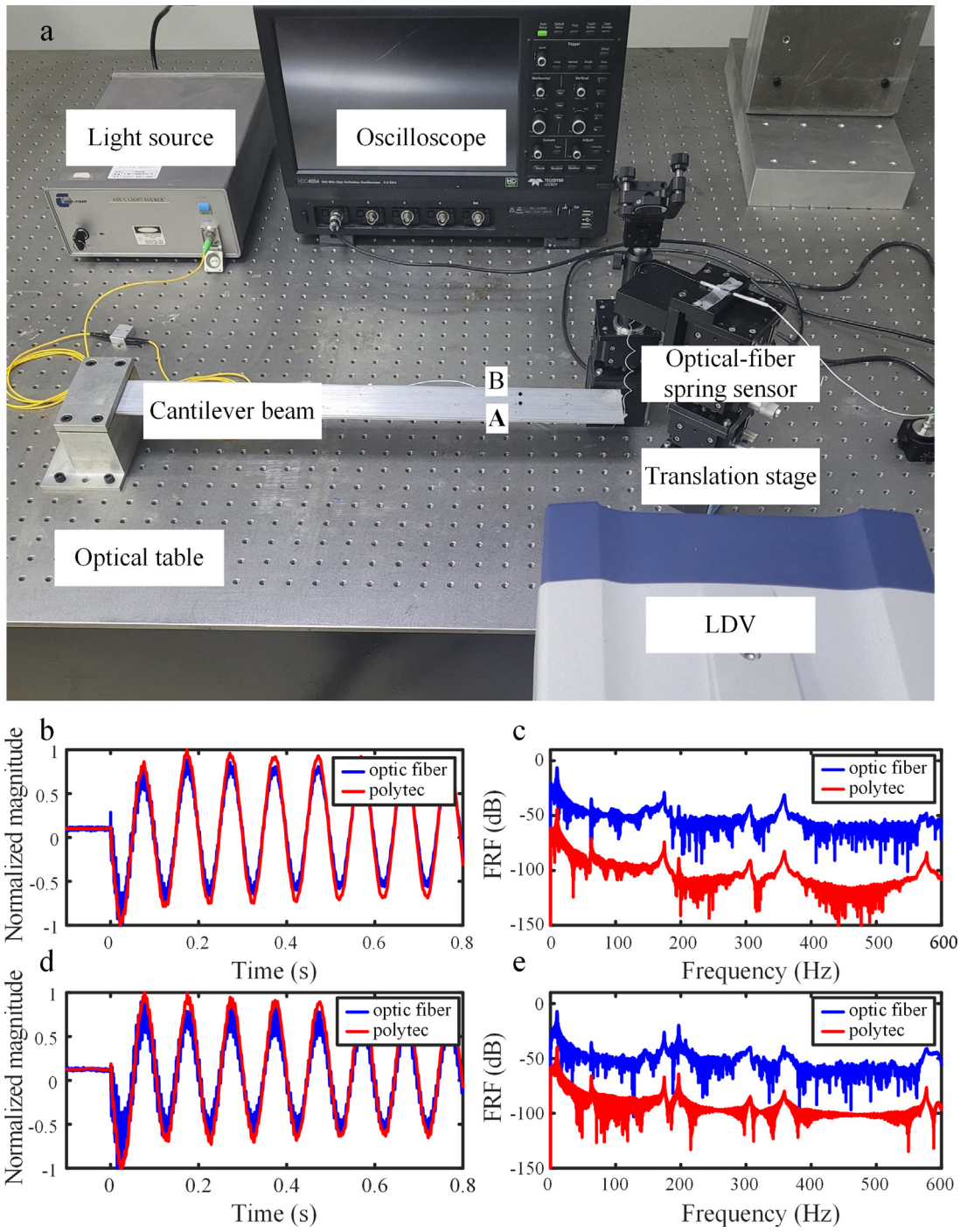

Fig. 3. (a) Cantilever beam vibration experiment arrangement. (b-c) When the excitation point is located at the beam center line, the vibration signal measured by the optical-fiber spring and the LDV and the corresponding frequency responses. (d-e) When the excitation point is located at the eccentric position, the vibration signal measured by the optical-fiber spring and the LDV and the corresponding frequency responses.

FBG sensor is demodulated by another FBG [39,40]. Respectively, while the point-wise FBG has the displacement sensitivity of 5 mV/nm. It should be noted that, the FBG proposed in Ref. [39,40] is very sensitive, accurate, and with a good linearity, compared to the proposed optical-fiber spring due to the fact that the proposed sensor is based on the large bending of the fiber. However, the proposed sensor can be used for a quick detection of the large deformations of flexible structures, although a pre-calibration is suggested. We also note that, if the fabrication condition, including the boundary condition and the gluing process, and the initial length of the optical-fiber spring is altered, the measuring range can be altered (and tuned) and thus a linearity calibration of the optical-fiber spring before the measurement is required. On the other hand, with the same fabrication conditions, the proposed optical-fiber spring is reproducible with the same coiling behavior.

3. Experiment and discussion

In order to demonstrate the ability for long-range displacement sensing, we measure the dynamic out-of-plane deflection of a cantilever beam with the proposed optical-fiber spring sensor.

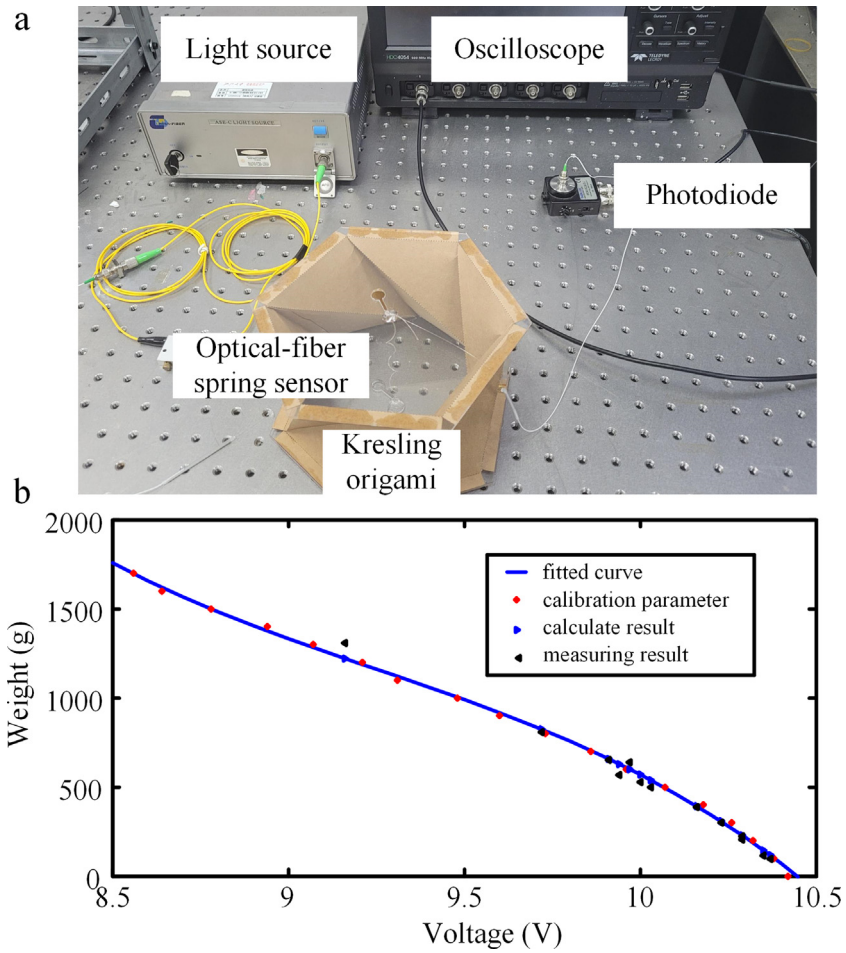

Fig. 4. (a) Force sensor measurement experiment arrangement. (b) Measured results and fitted curves. . (For interpretation of the references to color in this figure legend, the reader is referred to the web version of this article.)

The experimental setup is shown in Fig. 3a. The dimensions of the flexible cantilever beam, made of aluminum (6061), are 50 mm in width, 500 mm in length, and 3 mm in thickness. The beam was chosen long enough to have a large dynamic end displacement but short enough to avoid a significant static deflection due to its own weight. Also, the width of the beam is wider to allow a symmetric arrangement of the sensing points for calibrations and comparisons. One end of the cantilever beam was mounted on the optical table. The optical-fiber spring sensor was arranged at the right end, where one end of the optical-fiber spring was glued to a high vertical translation stage, composed of four standardized optical translation stages, and the other end was glued pointwisely to the cantilever beam. The integrated high vertical translation stage can be used to tune the initial length of the optical-fiber spring, where the desired region of linearity can be tuned before the measurement. The vibration of the beam was excited by the impact of a steel ball. By controlling the drop of the steel ball at a fixed height with an electromagnet, the repeatability of the stimulating loadings can be ensured in each experiment. A non-contact scanning laser Doppler vibrometer (LDV) system (PSV-500, Polytec, Waldbronn, Baden-Württemberg, Germany) was used to validate the sensing performance of the proposed optical-fiber spring sensor. The sensing locations for the two sensors (i.e., the optical-fiber spring and the LDV) on the beam are the same distance from the fixed end of the beam and are symmetrical to the center line of the beam.

The normalized transient displacement responses measured by the two sensors are shown in Fig. 3b, when the loading is excited at the central line (marked as “A” in Fig. 3a), and Fig. 3d, when the loading is excited off the central line (marked as “B” in Fig. 3a), and good agreements can be observed. The accuracy of the sensor, compared to the measurement result of the laser Doppler vibrometer, is about 70 μm. The corresponding frequency response curves are shown in Fig. 3c and e. The frequency responses also demonstrate good agreements between the two sensors. By performing a finite element analysis, the resonant frequencies in the frequency responses are obtained and are consistent with those of each vibrational mode of the cantilever beam. A comparison of the resonant modes of the cantilever beam are provided in Supplement 1. We note that the proposed optical-fiber spring, while being a contact-type sensor, contributes negligible loading effect to the detected structure to the spiral configuration. In addition, it should be noted that, the proposed optical-fiber spring, with a horizontal arrangement, has potential to be used to detect the in-plane vibrations of the flexible structures (e.g., here the cantilever beam) while the LDV cannot be used for comparison, unless a 3D LDV is used. The discussion of the reliability, consistency of the long-term operation, and the response time of the proposed optical-fiber spring are provided in Supplement 1.

In addition to serve as a sensor to measure dynamic displacement of structural vibrations or transient waves, the proposed optical-fiber spring can also be used to detect force, when being combined with appropriate mechanisms. In this letter, a *Kresling* origami was used to transfer the light loss in the optical-fiber spring to the force response. *Kresling* origami, as shown in Fig. 4a,

is a three-dimensional origami that shrinks under compression in the direction perpendicular to the two end panels and possesses good resilience after the loadings are released.

We can attach the two ends of the optical-fiber spring with the epoxy glue to the center of the upper and lower panels, each made of acrylic and with a central hole for gluing the fiber, of the *Kresling* origami, respectively. In this arrangement, the displacement of the compressed *Kresling* origami can be obtained by the optical-fiber spring and the applied force perpendicular to the two panels of the *Kresling* origami can be indirectly measured. The experimental setup on force sensing using the combination of the optical-fiber spring and the *Kresling* origami is shown in Fig. 4a. We first calibrated the force sensing ability by placing weights on the top panel of the *Kresling* origami. The data points used to calibrate are shown in the red rhombus in Fig. 4b. The experimental data were then fitted using Matlab and the fitting curve is the blue curve in Fig. 4b. Here, a cubic polynomial was adopted for curve fitting and the fitting result is shown in Eq. (1).

$$W = -210V^3 + 5840V^2 - 54700V + 174080, \tag{1}$$

where V is electrical signal of the photodiode. After calibration, different objects were placed on the surface of the top panel of the *Kresling* origami and the electrical signals are used to calculate their weights (blue triangle) and their true weights are marked as black triangle for comparison. The comparison results are shown in Fig. 4b. From the measurement results and the comparisons, we can see that a high-accuracy force sensing can be achieved based on the proposed optical-fiber spring.

4. Conclusions

In conclusion, inspired by tendril coiling, we introduce a mechanically-induced optical-fiber spring which can serve as sensors, based on the macro bending loss of optical fibers. The optical-fiber spring has good elasticity like a mechanical spring, which can be easily elongated or shortened to measure large displacement response with a negligible loading effect. In this letter, the vibration of the cantilever beam is measured and the results are compared with those obtained by the LDV. Furthermore, combined with the *Kresling* origami, the optical-fiber spring can also serve as a force sensor. The proposed optical-fiber spring inherits the advantages of strong anti-electromagnetic interference of optical fiber sensors and solves the disadvantages of small range and high loading effect of optical-fiber Bragg grating displacement sensors. The proposed optical-fiber spring sensor can be quickly fabricated to detect dynamic responses of the flexible structures or used as a load cell, and we note that it can be used as a tool to quickly determine the modes of the structure in frequency domain.

Declaration of competing interest

The authors declare no conflicts of interest.

Data availability

Data will be made available on request

Funding

Kuo-Chih Chuang gratefully acknowledges the financial support from the National Natural Science Foundation of China [Grant No. 11972318]. Yong Wang acknowledges the financial support from the National Natural Science Foundation of China [Grant Nos. 11872328 and 12132013]. Ronghua Huan acknowledges the financial support from the National Natural Science Foundation of China [Grant No. 12172323].

Appendix A. Supplementary data

Supplementary material related to this article can be found online at https://doi.org/10.1016/j.eml.2023.102032. See Supplement 1 for supporting content.

References

[1] C. Huang, Z. Wang, D. Quinn, S. Suresh, K.J. Hsia, Differential growth and shape formation in plant organs, Proc. Natl. Acad. Sci. 115 (2018) 12359.
[2] W. Wang, C. Li, M. Cho, S.-H. Ahn, Soft tendril-inspired grippers: shape morphing of programmable polymer–paper bilayer composites, ACS Appl. Mater. Interfaces 10 (2018) 10419.
[3] F. Klimm, S. Schmier, H.F. Bohn, S. Kleiser, M. Thielen, T. Speck, Biomechanics of tendrils and adhesive pads of the climbing passion flower Passiflora discophora, J. Exp. Bot. 73 (2022) 1190.
[4] G.M. Spinks, Advanced actuator materials powered by biomimetic helical fiber topologies, Adv. Mater. 32 (2020) 1904093.
[5] S.J. Gerbode, J.R. Puzey, A.G. McCormick, L. Mahadevan, How the cucumber tendril coils and overwinds, Science 337 (2012) 1087.
[6] G. Wan, C. Jin, I. Trase, S. Zhao, Z. Chen, Helical structures mimicking chiral seedpod opening and tendril coiling, Sensors 18 (2018) 2973.
[7] J. Liu, J. Huang, T. Su, K. Bertoldi, D.R. Clarke, Structural transition from helices to hemihelices, PLoS One 9 (2014) e93183.
[8] J. Huang, J. Liu, B. Kroll, K. Bertoldi, D.R. Clarke, Spontaneous and deterministic three-dimensional curling of pre-strained elastomeric bi-strips, Soft Matter 8 (2012) 6291.
[9] B.J. Cafferty, V.E. Campbell, P. Rothemund, D.J. Preston, A. Ainla, N. Fulleringer, A.C. Diaz, A.E. Fuentes, D. Sameoto, J.A. Lewis, Fabricating 3D structures by combining 2D printing and relaxation of strain, Adv. Mater. Technol. 4 (2019) 1800299.
[10] Y. Forterre, J. Dumais, Generating helices in nature, Science 333 (2011) 1715.
[11] S. Wang, Y. Gao, A. Wei, P. Xiao, Y. Liang, W. Lu, C. Chen, C. Zhang, G. Yang, H. Yao, Asymmetric elastoplasticity of stacked graphene assembly actualizes programmable untethered soft robotics, Nat. Commun. 11 (2020) 1.
[12] M. Koenigsdorff, J. Mersch, S. Pfeil, G. Gerlach, High-strain helical dielectric elastomer actuators, in: Proc. of SPIE Vol. 2022, 120420G.
[13] M. Wang, Y. Han, L.-X. Guo, B.-P. Lin, H. Yang, Photocontrol of helix handedness in curled liquid crystal elastomers, Liq. Cryst. 46 (2019) 1231.
[14] Z. Hu, Y. Li, J.-a. Lv, Phototunable self-oscillating system driven by a self-winding fiber actuator, Nat. Commun. 12 (2021) 1.
[15] V. Lutz-Bueno, S. Bolisetty, P. Azzari, S. Handschin, R. Mezzenga, Self-winding gelatin–amyloid wires for soft actuators and sensors, Adv. Mater. 32 (2020) 2004941.
[16] Z. Hu, Y. Li, T. Zhao, J.-a. Lv, Self-winding liquid crystal elastomer fiber actuators with high degree of freedom and tunable actuation, Appl. Mater. Today 27 (2022) 101449.
[17] M. Kanik, S. Orguc, G. Varnavides, J. Kim, T. Benavides, D. Gonzalez, T. Akintilo, C.C. Tasan, A.P. Chandrakasan, Y. Fink, Strain-programmable fiber-based artificial muscle, Science 365 (2019) 145.
[18] N. Kuse, A. Ozawa, Y. Kobayashi, Static FBG strain sensor with high resolution and large dynamic range by dual-comb spectroscopy, Opt. Express 21 (2013) 11141.
[19] R. Li, Y. Chen, Y. Tan, Z. Zhou, T. Li, J. Mao, Sensitivity enhancement of FBG-based strain sensor, Sensors 18 (2018) 1607.
[20] K.C. Chuang, C.C. Ma, C.Y. Wang, Free-edge sensor placement for identifying vibration modes of structures subjected to impact loadings using fiber Bragg gratings, Struct. Control Health Monit. 23 (2016) 1350.
[21] Z.-L. Xu, Y.-H. Wang, K.-C. Chuang, Spectral shaping of fiber Bragg gratings based on non-rigid origami, Opt. Lett. 46 (2021) 4825.
[22] J. Kumar, G. Singh, M.K. Saxena, O. Prakash, S.K. Dixit, S.V. Nakhe, Development and studies on FBG temperature sensor for applications in nuclear fuel cycle facilities, IEEE Sens. J. 21 (2020) 7613.
[23] B. Zhang, M. Kahrizi, High-temperature resistance fiber Bragg grating temperature sensor fabrication, IEEE Sens. J. 7 (2007) 586.
[24] N. Hirayama, Y. Sano, Fiber Bragg grating temperature sensor for practical use, ISA Trans. 39 (2000) 169.
[25] A.A. Abushagur, N. Arsad, M. Ibne Reaz, A. Ashrif, A. Bakar, Advances in bio-tactile sensors for minimally invasive surgery using the fibre Bragg grating force sensor technique: A survey, Sensors 14 (2014) 6633.
[26] L. Xiong, G. Jiang, Y. Guo, H. Liu, A three-dimensional fiber Bragg grating force sensor for robot, IEEE Sens. J. 18 (2018) 3632.
[27] P.L. Ko, K.C. Chuang, C.C. Ma, A fiber Bragg grating-based thin-film sensor for measuring dynamic water pressure, IEEE Sens. J. PP (2018) 1.
[28] C. Hong, Y. Zhang, L. Borana, Design, fabrication and testing of a 3D printed FBG pressure sensor, IEEE Access 7 (2019) 38577.

[29] K.C. Chuang, Z.Q. Zhang, H.X. Wang, Experimental study on slow flexural waves around the defect modes in a phononic crystal beam using fiber Bragg gratings, Phys. Lett. A 3963 (2016).
[30] T. Li, C. Shi, H. Ren, A novel fiber Bragg grating displacement sensor with a sub-micrometer resolution, IEEE Photon. Technol. Lett. 29 (2017) 1199.
[31] C. Li, L. Sun, Z. Xu, X. Wu, T. Liang, W. Shi, Experimental investigation and error analysis of high precision FBG displacement sensor for structural health monitoring, Int. J. Struct. Stab. Dyn. 20 (2020) 2040011.
[32] A. Harris, P. Castle, Bend loss measurements on high numerical aperture single-mode fibers as a function of wavelength and bend radius, J. Lightw. Technol. 4 (1986) 34.
[33] A. Goriely, M. Tabor, Spontaneous helix hand reversal and tendril perversion in climbing plants, Phys. Rev. Lett. 80 (1998) 1564.
[34] H. Zhao, X. Gao, Q. Qin, J. Wang, Formation of chiral morphologies of biological materials induced by chirality, Bioinspir. Biomimetics 16 (2021) 066005.
[35] R. Huang, Y. Xue, Z. Li, Z. Liu, Programmable spiral and helical deformation behaviors of hydrogel-based bi-material beam structures, Int. J. Struct. Stab. Dyn. 20 (2020) 2041010.
[36] T. McMillen, A. Goriely, Tendril perversion in intrinsically curved rods, J. Nonlinear Sci. 12 (2002) 241.
[37] Z. Chen, Shape transition and multi-stability of helical ribbons: a finite element method study, Arch. Appl. Mech. 85 (2015) 331.
[38] Z. Yang, Z. Zhai, Z. Song, Y. Wu, J. Liang, Y. Shan, J. Zheng, H. Liang, H. Jiang, Conductive and elastic 3D helical fibers for use in washable and wearable electronics, Adv. Mater. 32 (2020) 1907495.
[39] K.-C. Chuang, C.-C. Ma, Multidimensional dynamic displacement and strain measurement using an intensity demodulation-based fiber Bragg grating sensing system, J. Lightw. Technol. 28 (2010) 1897.
[40] K.-C. Chuang, C.-C. Ma, Tracking control of a multilayer piezoelectric actuator using a fiber Bragg grating displacement sensor system, IEEE Trans. Ultrason. Ferroelectr. Freq. Control 56 (2009) 2036.